Analysis of Networked Structural Control With Packet Loss

Thao H. T. Truong, *Graduate Student Member, IEEE*, Peter Seiler, *Member, IEEE*, and Lauren E. Linderman, *Member, IEEE*

***Abstract*— This brief considers the analysis of networked structural control systems with measurement loss. This is modeled as a sampled-data system that integrates the discrete-time operation of the controller with a fast-sampling approximation of the continuous-time structural (plant) dynamics. Random measurement loss in each channel due to the use of the wireless transmission is modeled as a Bernoulli process. This leads to a discrete-time, Markov jump linear model for the feedback system. An H_2-norm analysis is proposed to assess the stability and the performance of the structural control. An example of a three-story building model is used to illustrate this approach. The H_2-norm results are shown to be in agreement with the numerical simulations. The analysis can, thus, be used to assess various design choices. For example, the relationship between the probability of signal loss and the H_2-norm depends on the method used to handle the signal loss. Moreover, the analysis shows that, for a jump controller setup using steady-state Kalman gains, the system can become unstable at very small probabilities of signal loss.**

***Index Terms*— Earthquake engineering, Markov jump linear system, networked control system, packet loss, sampled-data system, stability, structural engineering.**

I. Introduction

CIVIL structures are vulnerable to dynamic deformation during natural hazards. Significant economic losses in past earthquakes due to structural damage have encouraged a transition to low-damage design, as opposed to focusing only on life safety. These tighter response requirements motivate the use of feedback structural control [1], [2].

Traditionally, the communication between the components of control systems is cabled. Compared to tethered systems, wireless networks offer potential flexibility and redundancy through applications of decentralized and adaptive control strategies [3], [4]. Wireless smart sensor platforms were originally developed for monitoring applications and have been successfully applied to bridge structures [5]. However, unlike monitoring applications, feedback control requires reliable and real-time measurements, which can be challenging due to signal loss and delay inherent in wireless communication. Therefore, the impact of signal loss and delay must be addressed for the successful implementation of wireless sensors in structural control.

Manuscript received February 3, 2020; revised July 26, 2020 and November 20, 2020; accepted December 28, 2020. Date of publication February 9, 2021; date of current version December 15, 2021. Manuscript received in final form January 11, 2021. This work was supported by NSF Award 1750225. Recommended by Associate Editor A. Speranzon. *(Corresponding author: Thao H. T. Truong.)*

Thao H. T. Truong and Lauren E. Linderman are with the Department of Civil, Environmental, and Geo- Engineering, University of Minnesota, Twin Cities, MN 55455 USA (e-mail: truon228@umn.edu; llinderm@umn.edu).

Peter Seiler is with the Department of Electrical Engineering and Computer Science, University of Michigan, Ann Arbor, MI 48109 USA (e-mail: pseiler@umich.edu).

Digital Object Identifier 10.1109/TCST.2021.3051578

Approaches for dealing with signal loss and delay include the utilization of decentralization, communication protocols, hardware/middleware design, and control algorithms. Decentralization limits the distance and the number of communication links by dividing the network into subsystems. This compromises the system knowledge available to the controller for improved communication performance [6]. Hardware/middleware design makes use of onboard computing and network utilization to reduce and provide tolerance to signal loss and delay [4], [7]–[9]. In addition, the wireless communication protocols, such as time-division multiple access (TDMA) and code-division multiple access (CDMA), can be tailored for civil engineering applications [4], [9], [10], and there often exists a tradeoff between latency and reliability while considering the optimal protocol [11]. Beyond improving the communication, control implementations directly account for delay and signal loss in the algorithms [12]–[15]. Previous work shows that different ways of handling signal loss affect system passivity [16], [17]. While holding the control command when the signal loss occurs [16] may inject additional energy to the system and cause a loss of passivity, dropping the command to zero [17] retains passivity.

Developers of wireless structural control often validate their design using limited experimental and numerical simulations [4], [7]–[9], [12]. A drawback of simulation-based methods is that the limited duration of earthquake excitations and the random occurrence of signal loss may not reflect the performance loss possible during the lifetime of the system and, therefore, underestimate the possible responses. Within the controls community, the mathematical analyses for system norms, such as $\mathbf{H}_2$-norm and $\mathbf{H}_\infty$-norm, are often used as the system performance evaluations, which could be alternatives for the simulation-based methods. The $\mathbf{H}_2$-norm of a linear time-invariant system can be interpreted as the gain from the white noise disturbance to the steady-state variance of the output. Earthquake response analysis often leverages a filtered random disturbance [18], [19] as real earthquake excitations are highly random and wideband. Therefore, the $\mathbf{H}_2$-norm is the suitable choice for the performance criterion. Wireless feedback control introduces packet drops that are both time-varying and random. The standard $\mathbf{H}_2$-norm must be adapted to address both of these effects.

The key contribution of this brief is to assess the performance of wireless structural control systems using an adapted version of the $\mathbf{H}_2$-norm, which considers the effects of signal loss and slow sampling time. The proposed $\mathbf{H}_2$-norm analysis method is based on the Lyapunov stability theorem. The analysis follows two steps: modeling of the lossy,

slow-sampled system and solving the Lyapunov equation. Markov jump linear systems' theory [20] and sampled-data systems' theory [21], [22] are employed for the modeling. The $\mathbf{H}_2$-norm is obtained by solving the set of Lyapunov equations associated with the jump model. The analysis method is applied to study the stability and performance of a controlled building. The outcome of the analysis relates the probability of signal loss and the sampling time to the $\mathbf{H}_2$-norm. This can be used to assess the design tradeoff between sampling time and signal reliability.

II. Formulation of the Controlled Systems

A. Feedback Control of Structures

In this brief, we consider the feedback control of a building structure for mitigating the earthquake response. The structure (the plant) $\mathcal{P}$ is controlled by actuators placed on each floor. The feedback control system consists of the sensors that measure the building response, the centralized controller $\mathcal{C}$ that computes the control command using the measurement from the sensors, the actuators that execute the control command, and the communication links between the components to transfer all the required data. During earthquakes, the building deformation, specifically, the interstory drifts (unitless ratio calculated by the difference in horizontal displacements of two adjacent floors divided by the floor height) is to be limited by the control system.

In continuous time, the horizontal displacement and velocity of the floors relative to the ground together form the state vector $x(t) \in \mathbb{R}^{n_x}$. To detect the building response, the measured response vector $y(t) \in \mathbb{R}^{n_y}$ (floor horizontal accelerations or full-state measurements) is gathered by n_y sensors placed on the structure at each level. The building is subjected to the earthquake loading, which is modeled by the ground acceleration, $a(t) \in \mathbb{R}$. Unless the statistical data about the frequency content and the duration of the targeted earthquakes are available to generate synthetic ground motions, a white noise can be a sufficiently suitable input model [23]. In this work, a band-limited white noise with a 400-Hz bandwidth is considered for the earthquake input. The structure is also excited by the actuators, which generates n_u actuator forces denoted by the input vector $u(t) \in \mathbb{R}^{n_u}$. The state-space representation of the building is given as follows:

$$\mathcal{P}: \begin{cases} \dot{x}(t) = Ax(t) + B_1 a(t) + B_2 u(t) \\ z(t) = C_z x(t) \\ y(t) = C_y x(t) + D_y u(t) \end{cases} \tag{1}$$

where $z(t) \in \mathbb{R}^{n_z}$ is the vector containing the controlled responses of the structure, which are the interstory drifts.

The building dynamics are in continuous time, but the controller is implemented in discrete time. Let $x_s[k]$, $u_s[k]$, and $y_s[k]$ be the discrete-time companions of $x(t)$, $u(t)$, and $y(t)$, respectively. $x_s[k]$ and $y_s[k]$ are obtained by sampling $x(t)$ and $y(t)$ with time step T_s. The controller updates the required actuator forces at discrete time instances, denoted as $u_s[k]$. A zero-order hold is used between sample times to generate $u(t)$.

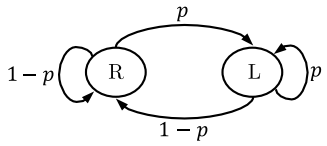

Fig. 1. Bernoulli process of the signal loss on each channel.

B. Wireless Sensor Network and Signal Loss

For a controlled structure that uses a wireless sensor network for measurement feedback, the controller sampling rate will be limited, predominantly by the communication latency of the transceivers. A typical guideline for the selection of the sampling time is about ten times faster than the system bandwidth and never less than two times the frequency that needs to be observed [24, Sec. 8.8]. However, such a fast sampling time is difficult to achieve in this centralized, wireless structural control setting. As seen in [3], the sampling period in the case study was limited to 0.08 s (12.5-Hz sampling frequency) for the centralized wireless control system of the three-story structure. Such a slow sampling time has significant effects on the closed loop. In this brief, the results for $T_s = 0.02$ s and $T_s = 0.05$ s are presented.

Signal loss causes random changes in the dynamics of the model visible to the controller. Under assumptions about the stochastic process governing the occurrence of signal loss, the system can be modeled as a Markov jump linear system, a class of time-varying models that can switch between multiple linear modes following a Markov chain process. A single measurement can be either lost (L) or received (R) during the transmission for the network to be studied, so the total number of Markov modes with n_c channels is 2^{n_c}. We assume that each channel is lost with probability p or received with probability $1 - p$ (see Fig. 1) at the receptor following an independent identically distributed (i.i.d) Bernoulli process [25]. Time-varying network performance captured by fading models [14], e.g., network dropout due to the environment as in vehicle control, is not a significant concern for building control. That being said, a fading model could be incorporated within this analysis framework. The Bernoulli process, however, is sufficient for modeling the signal loss in the wireless structural control problems.

The lossy, individual channels of the sampled system are captured by partitioning the received measurement vector. Let $y_s[k] = [y_{s,1}[k]^T \;\; y_{s,2}[k]^T \;\; \cdots \;\; y_{s,n_c}[k]^T]^T$ be the sample of the measured response, $y(t)$, at the kth time step. $y_s[k]$ is partitioned so that the signals sent in the same channel are grouped together. The received measurement is $y_r[k] = \left[y_{r,1}[k]^T \; y_{r,2}[k]^T \cdots y_{r,n_c}[k]^T\right]^T$. The lossy signal received by the cth channel ($c = 1, 2, \ldots, n_c$) is modeled as $y_{r,c}[k] = \theta_c[k] \times y_{s,c}[k]$, where $\theta_c[k]$ is the binary variable modeling the loss process ($\theta_c[k] = 0$: lost; $\theta_c[k] = 1$: received). For the building structure in this work, each channel transmits the measurements from one floor. The number of channels, n_c, is also the number of floors of the building.

In this brief, we investigate the jump controllers that switch between predefined modes. Let $\theta[k] = \left[\theta_1[k], \theta_2[k], \ldots, \theta_{n_c}[k]\right]^T$ be the binary array containing the

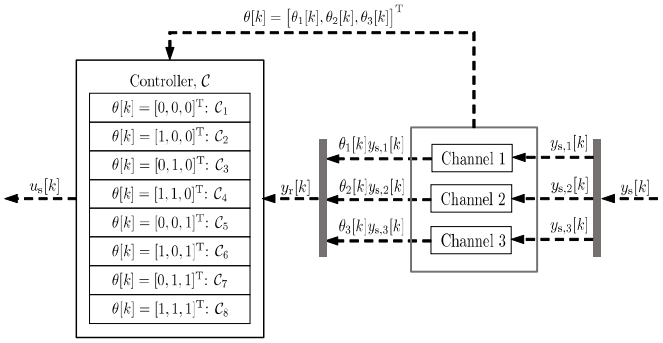

Fig. 2. Signal loss and jump controller (three wireless channels and eight controller modes).

reception information of all channels at the time step k. The switching logic of the controller depends on $\theta[k]$, which is known by the controller (see Fig. 2).

C. Numerical Building Model

The structure in this study is the three-story benchmark model that is described by Ohtori *et al.* [26]. The structure is a steel building with dimensions 36.58 m × 54.87 m in plan and 11.89 m in elevation (see Fig. 3). Designed for seismic research, the structure is commonly used to investigate structural control strategies. The benchmark supports both linear and nonlinear simulations. The linear version is used in this work. The initial benchmark model has 33 degrees of freedom. The Guyan condensation [27] is used to reduce the complexity of the model for the control design. The linear condensed model has 3 degrees of freedom, which are the horizontal displacements of the floors. The natural frequencies of the simulated model are 0.99, 3.06, and 5.83 Hz.

The dynamic model of the controlled structure subjected to ground acceleration is given by the equation of motion

$$M\ddot{\chi}(t) + C\dot{\chi}(t) + K\chi(t) = Ga(t) + Hu(t) \tag{2}$$

where $\chi(t)$, $\dot{\chi}(t)$, and $\ddot{\chi}(t) \in \mathbb{R}^3$ are vectors of horizontal displacements, velocities, and accelerations of the floors relative to the ground, $M, C,$ and $K \in \mathbb{R}^{3\times3}$ are mass, damping, and stiffness matrices of the structure, respectively, $G \in \mathbb{R}^3$ is the loading vector for the ground acceleration, and $H \in \mathbb{R}^{3\times3}$ is the loading matrix for the actuator forces. M, C, K, G, and H are given in Appendix A. Let the state vector of the continuous-time plant be

$$x(t) = \begin{bmatrix} \chi(t) \\ \dot{\chi}(t) \end{bmatrix}$$

and the state-space matrices of the plant are as follows:

$$A = \begin{bmatrix} 0 & I \\ -M^{-1}K & -M^{-1}C \end{bmatrix}$$
$$B_1 = \begin{bmatrix} 0 \\ M^{-1}G \end{bmatrix}, \quad B_2 = \begin{bmatrix} 0 \\ M^{-1}H \end{bmatrix}$$
$$C_z = \begin{bmatrix} \frac{1}{h_1} & 0 & 0 \\ -\frac{1}{h_2} & \frac{1}{h_2} & 0 \\ 0 & -\frac{1}{h_3} & \frac{1}{h_3} \end{bmatrix}, \quad D_z = 0 \tag{3}$$

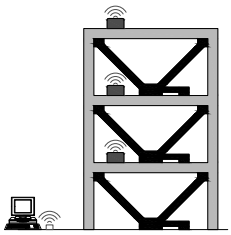

Fig. 3. Three-story building model.

where h_1, h_2, and h_3 are the story heights. C_y and D_y define the measured responses. For full-state feedback (measure the relative displacements and velocities)

$$C_y = I, \quad D_y = 0. \tag{4}$$

For absolute floor acceleration feedback

$$C_y = \begin{bmatrix} -M^{-1}K & -M^{-1}C \end{bmatrix}, \quad D_y = \begin{bmatrix} M^{-1}G \end{bmatrix}. \tag{5}$$

D. Control Laws

Three different control laws are evaluated. The first control law, LQRonoff, uses a linear quadratic regulator (LQR) with full-state feedback (measures the floor horizontal displacements and velocities). When a subset of the state feedback from a floor is lost, it will be replaced by zeros in the regulator.

The second control law, LQRhold, also uses a full-state feedback LQR but replaces the lost measurements with the previously received values. The initial state-feedback for LQRhold is $0_{n_x\times1}$.

The third control law to be considered, LQGswitch (Appendices C and E), employs the linear quadratic Gaussian (LQG) algorithm that combines the same LQR design from the full-state feedback cases with a switch estimator. LQGswitch uses the floor horizontal, absolute acceleration for feedback. The switch estimator has a propagation/correction form, where the corrector gain varies between 2^{n_c} modes. For each mode, a subset of the measurements vector is received by the controller, and the corrector gain is the steady-state Kalman gain solution computed on that subset of measurements. Note that while this "*ad hoc*" control law is simple to come up with, it is not an optimal solution. Switching between the corrector gains potentially leads to stability issues, which are shown and discussed in Section IV.

The design parameters of the LQR and the Kalman estimator are given in Appendix B.

The goal of the control is to limit the impact of the earthquake input on the interstory drift output of the building. The performance can be evaluated by the power gain from the input to the output. The metrics that we want to compute can be approximated by simulating the linear model with a noisy input and measuring the output variance. The analysis method, as presented in Section III, allows the expectation at the infinite time of this power gain to be evaluated without Monte Carlo simulations; the $\mathbf{H}_2$-norm of the system is the square root of this input–output power gain.

III. Modeling and $\mathbf{H}_2$-Norm Analysis

This section introduces the modeling and $\mathbf{H}_2$-norm analysis of the closed loop with signal loss. A continuous-time model and a discrete-time controller are combined using the sampled-data system theory [21], [22]. The closed loop is identified as a jump system, where the switching depends on the reception of measurement. Upon the sampled-data jump model, $\mathbf{H}_2$-norm analyses can be carried out by solving the associated Lyapunov equation.

A. Sampled-Data Systems

Given a continuous-time controlled structure and a control system running with a slow sampling time, T_s, the closed loop is identified as a sampled-data system. The technique [21] is a precise way to build a model with sampling time T_s for this class of systems (see Fig. 4). Instead of directly connecting a continuous-time plant and a discrete-time controller, the plant is first approximated by a fast-sampled discrete-time model with a time step T_f. In the lifting technique, two discrete-time subsystems with different sampling times are connected to form a closed loop that captures the response of the fast plant. A small T_f ensures the accuracy of the approximation. We used $T_\mathrm{f} = 0.0025$ s, which is more than 50 times faster than the dynamics of the plant. Note that T_f must be a divisor of T_s

$$T_\mathrm{s} = NT_\mathrm{f} \quad \text{with} N \in \mathbb{Z}^+. \tag{6}$$

With the approximate plant, the controller samples and sends a new command every N steps [see Fig. 4(b)].

The fast-sampled plant model for the building is

$$\mathcal{P}_\mathrm{f}: \begin{cases} x_\mathrm{f}[k_\mathrm{f}+1] = A_\mathrm{f}x_\mathrm{f}[k_\mathrm{f}] + B_{\mathrm{f},1}a_\mathrm{f}[k_\mathrm{f}] + B_{\mathrm{f},2}u_\mathrm{f}[k_\mathrm{f}] \\ z_\mathrm{f}[k_\mathrm{f}] = C_z x_\mathrm{f}[k_\mathrm{f}] \\ y_\mathrm{f}[k_\mathrm{f}] = C_y x_\mathrm{f}[k_\mathrm{f}] + D_y u_\mathrm{f}[k_\mathrm{f}] \end{cases} \tag{7}$$

where $B_{\mathrm{f},1} = \int_0^{T_\mathrm{f}} e^{A\tau}B_1 \; d\tau$, $B_{\mathrm{f},2} = \int_0^{T_\mathrm{f}} e^{A\tau}B_2 \; d\tau$, and $A_\mathrm{f} = e^{AT_\mathrm{f}}$.

Stacking the input and output of the fast-sampled plant and formulating the state-space model (see Appendix D) creates an equivalent approximation but with time step T_s [see Fig. 4(c)]. The equivalent plant (lifted plant)

$$\mathcal{P}_\mathrm{s}: \begin{cases} x_\mathrm{s}[k+1] = A_\mathrm{s}x_\mathrm{s}[k] + B_{\mathrm{s},1}a_\mathrm{s}[k] + B_{\mathrm{s},2}u_\mathrm{s}[k] \\ z_\mathrm{s}[k] = C_{\mathrm{s},z}x_\mathrm{s}[k] + D_{\mathrm{s},z1}a_\mathrm{s}[k] + D_{\mathrm{s},z2}u_\mathrm{s}[k] \\ y_\mathrm{s}[k] = C_y x_\mathrm{s}[k] + D_y u_\mathrm{s}[k] \end{cases} \tag{8}$$

where $x_\mathrm{s}[k]$ and $y_\mathrm{s}[k]$ are sampled from $x_\mathrm{f}[k_\mathrm{f}]$ and $y_\mathrm{f}[k_\mathrm{f}]$, respectively

$$x_\mathrm{s}[k] = x_\mathrm{f}[N(k-1)+1], \quad y_\mathrm{s}[k] = y_\mathrm{f}[N(k-1)+1]. \tag{9}$$

The earthquake acceleration input, $a_\mathrm{f}[k_\mathrm{f}]$, and the controlled response output, $z_\mathrm{f}[k_\mathrm{f}]$, of the fast-sampled system are arranged into the stacked input, $a_\mathrm{s}[k]$, and stacked output, $z_\mathrm{s}[k]$, respectively

$$a_\mathrm{s}[k] = \begin{bmatrix} a_\mathrm{f}[N(k-1)+1] \\ a_\mathrm{f}[N(k-1)+2] \\ \cdots \\ a_\mathrm{f}[Nk] \end{bmatrix} \tag{10}$$

$$z_\mathrm{s}[k] = \begin{bmatrix} z_\mathrm{f}[N(k-1)+1] \\ z_\mathrm{f}[N(k-1)+2] \\ \cdots \\ z_\mathrm{f}[Nk] \end{bmatrix}. \tag{11}$$

The control forces are held during each control time step

$$u_\mathrm{f}[kN+1] = u_\mathrm{f}[kN+2] = \cdots = u_\mathrm{f}[kN+N] = u_\mathrm{s}[k]. \tag{12}$$

Given the slow-sampled equivalent model of the structure, $\mathcal{P}_\mathrm{s}$, and the control system, $\mathcal{C}$, both with sampling time T_s,

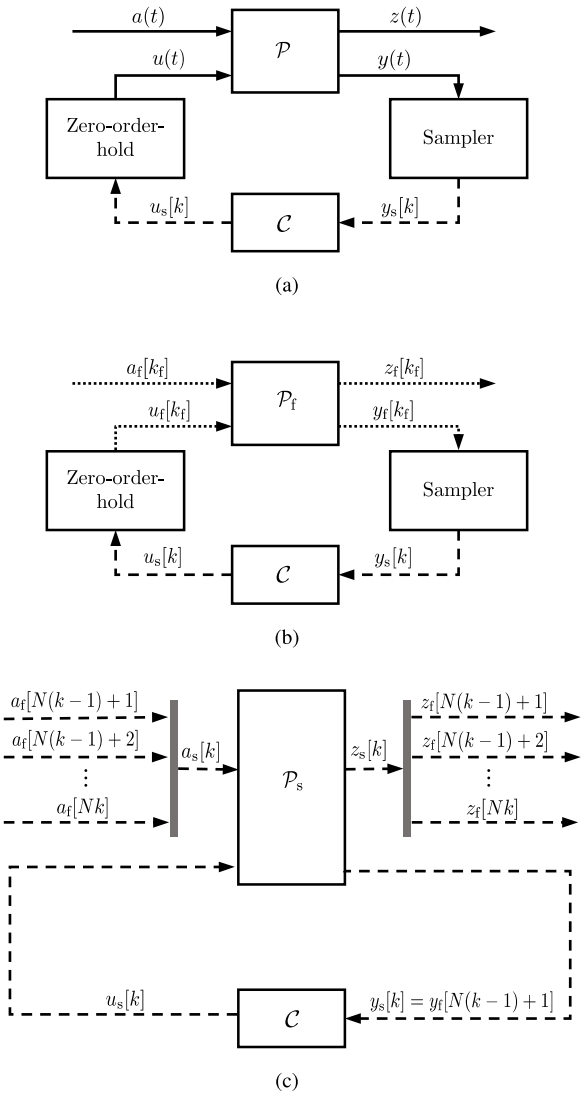

Fig. 4. Formulation of the analysis model using the lifting technique (solid lines: continuous-time signals; dashed lines: discrete-time signals with sampling time T_s; and dotted lines: discrete-time signals with sampling time T_f). (a) Closed loop with the continuous-time plant, $\mathcal{P}$, and slow-sampled controller, $\mathcal{C}$. (b) With the fast-sampled plant, $\mathcal{P}_\mathrm{f}$. (c) With the lifted plant, $\mathcal{P}_\mathrm{s}$.

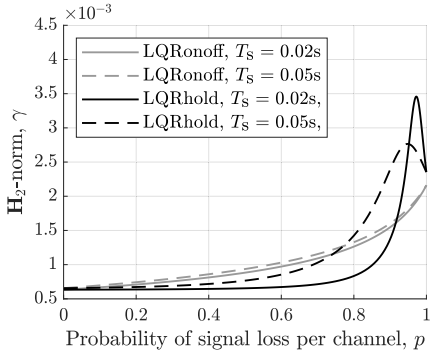

Fig. 5. $\mathbf{H}_2$-norm for LQRonoff and LQRhold.

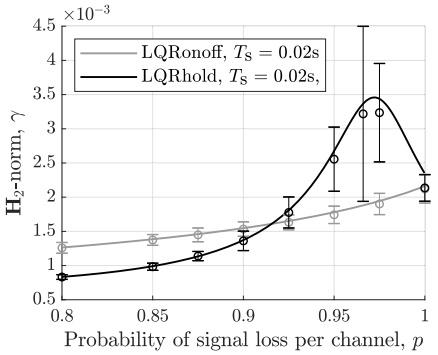

Fig. 6. Comparison between simulation result (error bars) and analysis result (curves).

the closed-loop model, $\mathcal{G}$, can be obtained by linear fractional transformation (lft).

B. Jump System and $\mathbf{H}_2$*-Norm*

While the building model is linear time-invariant, the control system varies due to the loss of the measurements (see Section II-B) and the switching controller upon the detection of signal loss (see Section II-D). Considering the plant $\mathcal{P}_s$ and the jump controller $\mathcal{C}$ that switches between n_m modes, $\{\mathcal{C}_1, \mathcal{C}_2, \ldots, \mathcal{C}_{n_m}\}$ (see Fig. 2), the closed-loop system [see Fig. 4(c)] becomes a Markov jump linear system of n_m modes $\{\mathcal{G}_1, \mathcal{G}_2, \ldots, \mathcal{G}_{n_m}\}$

$$\mathcal{G}_i = \text{lft}(\mathcal{P}_s, \mathcal{C}_i) \text{ for } i = 1, 2, \ldots, n_m. \tag{13}$$

Let $V = \{v_1, v_2, \ldots, v_{n_m}\}$ be the unconditional probability distribution of the Markov modes, $P = \{q_{ij}\}$ $(i, j = 1, 2, \ldots, n_m)$ be the Markov transition matrix, and $\alpha[k] \in \{1, 2, \ldots, n_m\}$ denote the mode of the closed loop at any time step k

$$v_j = \Pr\{\alpha[k] = j\} \tag{14}$$

$$q_{ij} = \Pr\{\alpha[k+1] = j \mid \alpha[k] = i\}. \tag{15}$$

For the systems studied in this brief, the signal loss on each channel follows a Bernoulli process with probability p, and the probability distribution of the Markov mode at any time step is independent of the previous time step. Therefore, $q_{1j} = q_{2j} = \cdots = q_{n_m j} = v_j$ (for $j = 1, 2, \ldots, n_m$). The values of v_j's depend on p (see Appendix E).

The square of the $\mathbf{H}_2$-norm, γ^2, is the expectation of the power of the impulse response over all possible sequences

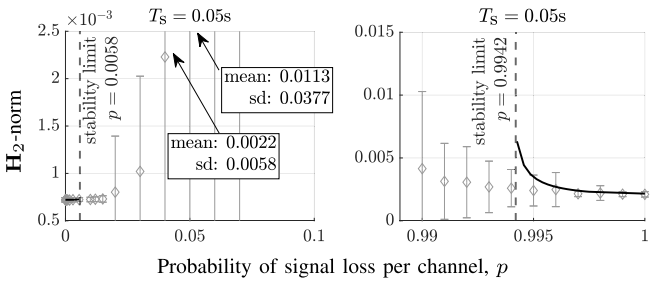

Fig. 7. LQGswitch simulation result (error bars), analysis result (curves), and stability limit of p (dashed lines).

of signal loss, as defined in [20, Definition 4.7]. An equivalent interpretation of the $\mathbf{H}_2$-norm squared is the expected infinite-time input–output power gain from an i.i.d white noise input over all possible signal loss sequences.

Let $[A_{\text{cl},i},\ B_{\text{cl},i},\ C_{\text{cl},i},\ D_{\text{cl},i}]$ denote the state-space representation of $\mathcal{G}_i$. We compute the $\mathbf{H}_2$-norm from the observability Grammians [see (16) and (17)] as presented in [20, eq. 4.40 and Prop. 4.8]. The observability Grammians are found by solving the set of n_m Lyapunov equations

$$Y_i = A_{\text{cl},i}^{\text{T}} \sum_{j=1}^{n_m} \left(q_{ij} Y_j\right) A_{\text{cl},i} + C_{\text{cl},i}^{\text{T}} C_{\text{cl},i} \ \ (i = 1, 2, \ldots, n_m) \tag{16}$$

where Y_i's are the expectations of the observability Grammians of the ith mode of the closed loop. These are linear equations of Y_i's. A positive definite solution to all Y_i's exists when the system is mean-square stable [28]. The $\mathbf{H}_2$-norm, γ, is computed from

$$\gamma^2 = \text{Tr} \sum_{i=1}^{n_m} \left(v_i \left(B_{\text{cl},i}^{\text{T}} \sum_{j=1}^{n_m} (q_{ij} Y_j) B_{\text{cl},i} + D_{\text{cl},i}^{\text{T}} D_{\text{cl},i} \right) \right). \tag{17}$$

IV. Result

This section discusses the outcome of the $\mathbf{H}_2$-norm analysis of the controlled three-story building. The analyses are conducted to assess the performance of the three control laws: LQRhold, LQRonoff, and LQGswitch. Many factors affect the relationship between the performance and the probability of signal loss, including: 1) how the signal loss is handled and 2) the sampling rate of the controller. The $\mathbf{H}_2$-norm analysis reflects the performance as a function of all the abovementioned factors. In addition, the agreement between the analysis result and the Monte Carlo simulation is persuasive that the analysis method can be used as an alternate tool for evaluating the effectiveness of the wireless structural control system.

A. Performance Evaluation Using the $\mathbf{H}_2$*-Norm*

The impact of different ways of handling signal loss on the $\mathbf{H}_2$-norm is shown in Fig. 5. In the figure, the $\mathbf{H}_2$-norms of LQRonoff and LQRhold at two different sampling times, $T_s = 0.02$ s and $T_s = 0.05$ s, are plotted as a function of the probability of signal loss. At small probabilities, $p < 0.2$, the difference between the four curves is negligible. When $p > 0.2$, the different effects of the two control laws are clearly evident. Comparing LQRonoff and LQRhold, the former has the $\mathbf{H}_2$-norm monotonically degrade with the increase of probability of signal loss, while the latter has a drastic

degradation of $\mathbf{H}_2$-norm at a high loss. The performance of LQRhold is better than LQRonoff up to high probabilities of packet loss ($p < 0.76$ for $T_s = 0.05$ s and $p < 0.92$ for $T_s = 0.02$ s) but can be even worse than the uncontrolled system at higher loss rates. These results appear to be related to prior work on networked systems. Specifically, it has been observed, under slightly different technical formulations, that passivity is retained when the control command is dropped to zero after a packet drop [17], while passivity is lost if the control command is held at its prior value [16]. Complete loss of the measurements ($p = 1$) brings both LQRonoff and LQRhold to the uncontrolled case, where there are no control forces. For LQRonoff, when a part of the state feedback is lost, the impact of the control lies between the fully controlled and the uncontrolled cases. However, for LQRhold, the consecutive losses interspersed with the occasional receipts of the measurement result in a large amount of energy injected into the system. This is more likely to have a significant impact when the time between the successful receptions is long. Therefore, the performance no longer degrades monotonically, and the peak of the $\mathbf{H}_2$-norm takes place as p is close to 1.

The analysis results also illustrate the impact of sampling time. In Fig. 5, $\mathbf{H}_2$-norms of LQRonoff with $T_s = 0.02$ s and $T_s = 0.05$ s are almost equal. However, the $\mathbf{H}_2$-norm of LQRhold is strongly dependent on T_s. LQRhold with $T_s = 0.02$ s clearly outperforms the same control laws with $T_s = 0.05$ s at $p < 0.95$.

B. Simulation Versus Analysis Result

Simulations are conducted to validate the analysis results. The simulations are performed with the closed-loop system excited by a random white noise input for 200 s. The simulation length is selected based on a typical earthquake duration. We compute the empirical $\mathbf{H}_2$-norm for each simulation. This is defined as the ratio of the root mean square (rms) of the norm of the interstory drift vector and the rms of the input white noise. An empirical estimate of the $\mathbf{H}_2$-norm is obtained by averaging over 100 simulations. The empirical estimate and the analysis result are compared in Fig. 6. Two control laws, LQRonoff and LQRhold with $T_s = 0.02$ s, are shown. For both cases with $p < 0.8$, the standard deviation of the empirical $\mathbf{H}_2$-norm is small (less than 6.3% of the mean), and the analysis result is in strong agreement with the mean value. At $p > 0.8$, the LQRonoff maintains this good agreement. For LQRhold, when p is near the extremal point, the empirical $\mathbf{H}_2$-norm has a very high variance (40% of the mean value at $p = 0.966$). Note that the analysis efficiently provides the expected value of the $\mathbf{H}_2$-norm considering all possible scenarios over an infinite horizon but does not capture the variation of the performance. The simulations, on the other hand, capture the variance of the empirical $\mathbf{H}_2$-norm. The high standard deviation of the empirical $\mathbf{H}_2$-norm given by the simulations shows that the performance of LQRhold at $0.95 < p < 1$ is strongly influenced by the loss sequence.

C. Stability of the Closed Loop

A finite $\mathbf{H}_2$-norm indicates the system is (mean-square) input–output stable, while an infinite $\mathbf{H}_2$-norm indicates system instability. A time-varying system jumping between stable modes may be unstable. Fig. 7 shows that, for LQGswitch and $T_s = 0.05$ s, between $p = 0.0058$ and $p = 0.9942$, the system is unstable. The results for $T_s = 0.02$ s (not shown in the figure) mirror those of $T_s = 0.05$ s. For $T_s = 0.02$ s, the destabilizing range of p has the lower limit at 0.0058 and the upper limit is even closer to 1. Note that all modes are stable when considered as standalone systems. The fact that the jump system is stable for both uncontrolled ($p = 1$) and no-loss controlled ($p = 0$) cases but becomes unstable when switching between stable modes ($0 < p < 1$) suggests that implementation of a control law requires careful evaluation of the destabilizing effect of signal loss.

In addition, as can be seen in Fig. 7, for a stable LQGswitch, $T_s = 0.05$ s and $p \notin (0.0058, 0.9960)$, the simulation mean aligns with the analysis result. For p in the middle of the destabilizing range ($0.06 < p < 0.98$), the simulation and analysis also agree on the instability (very large empirical $\mathbf{H}_2$-norm from the simulations). However, when p is close to the destabilizing limit, the simulations may not capture the unstable response. For example, with $T_s = 0.02$ s and for $p = 0.02$, the analysis detects instability, but the simulations return a finite average value of the empirical $\mathbf{H}_2$-norm less than the stable uncontrolled $\mathbf{H}_2$-norm. There are extreme sequences of loss and reception of signal that increases the variance of the output response to very high values. The combination of the probability of these extreme sequences and their amplification effect on the output response dictates the mean-square stability. There are cases in which the probabilities of these extreme sequences are too small that they are unlikely to occur in the finite-time simulations, but the amplification is large enough so that, if the simulations could be run forever, the expected input-to-output power gain would eventually go to infinity. While the simulations are unable to identify such cases, the analysis approach will be able to effectively capture the instability.

The source of instability of LQGswitch is the use of the steady-state Kalman gains that are not optimized for the estimation with intermittent observation. The necessary condition for the stability of the estimator is the convergence of the expectation of the predicted estimation error covariance [14]. By propagating the expected error covariance, which can be computed ahead of time for this i.i.d. switching estimator, we obtain the same destabilizing thresholds for p.

D. Application of the Analysis Method

While the performance of the controlled system depends on the probability of signal loss and the sampling time, there is no specific rule governing the performance. In fact, each control law has a different pattern for the relationship between the probability of signal loss, sampling time, and the $\mathbf{H}_2$-norm. The analysis method, therefore, is useful in selecting the best among a finite set of control laws, given prior knowledge about the signal loss. For example, Fig. 5 shows that LQRhold results in better $\mathbf{H}_2$-norm than LQRonoff for $p < 0.6$.

In addition, the analysis shows the sensitivity of the performance to signal loss and sampling time. For example, LQRhold can maintain the performance of less than 5%

increase in $\mathbf{H}_2$-norm up to $p = 0.58$ for $T_s = 0.02$ s, while, for $T_s = 0.05$ s, only up to $p = 0.15$ (see Fig. 5). In practice, there is often a bandwidth constraint that prevents simultaneously improving the sampling time and decreasing the probability of signal loss. From the analysis results, designers can choose whether to prioritize faster sampling time or lower signal loss in the implementation of the control algorithm.

V. Conclusion

This study considered the use of $\mathbf{H}_2$-norm analysis in performance and stability evaluation of networked controlled systems with signal loss. A significant concern while designing a wireless control system is the combinatory effects of signal loss and sampling time on system performance. The analysis method presented in this brief addressed that concern. At the core of the analysis method is the use of the Markov jump linear systems' theory to account for signal loss and the sampled-data systems' theory to account for the sampling time.

The analysis was specifically applied to the problem of wireless control of building structures. Observation from the case study on a three-story building model includes the effects of different ways of handling the measurement loss on the performance, the influence of sampling time, and the instability caused by signal loss.

The proposed analysis method can quantify the relationship between signal loss and performance. The use of a specific control law will lead to a unique signal-loss-to-performance relation; therefore, the method can be an efficient tool for selecting the best among a set of control laws. In addition, the analysis can be used as a stability assessment tool, which clearly shows the limiting probability of signal loss at which the system became unstable. In some cases, the corresponding simulations did not capture the instability, specifically when the probability of signal loss was close to the instability thresholds. With a finite simulation time and transient system variation due to high signal loss rate, the empirical $\mathbf{H}_2$-norm from the simulations might not approach the true value of the $\mathbf{H}_2$-norm. On the other hand, the simulation approach is still useful, as the variance of the empirical $\mathbf{H}_2$-norm can tell whether the performance of the system at a specific value of the probability of signal loss is reliable or not.

Future work will explore the application of the proposed analysis method in a reliability-based design framework for structural control, in which, traditionally, simulation-based methods are used for performance assessment. Incorporating the $\mathbf{H}_2$-norm analysis potentially reduces the required computational resources and, more importantly, captures the expected performance independent of a specific signal loss sequence.

Appendix A
Parameters of the Three-Story Building Model

$$M = \text{diag}([478350 \;\; 478350 \;\; 517790]) \text{ (kg)} \tag{18}$$

$$C = 1.0\text{e}+5 \times \begin{bmatrix} 7.7626 & -3.7304 & 0.6514 \\ -3.7304 & 5.8284 & -2.0266 \\ 0.6514 & -2.0266 & 2.4458 \end{bmatrix} \text{ (Ns/m)} \tag{19}$$

$$K = 1.0\text{e}+8 \times \begin{bmatrix} 4.3651 & -2.3730 & 0.4144 \\ -2.3730 & 3.1347 & -1.2892 \\ 0.4144 & -1.2892 & 0.9358 \end{bmatrix} \text{ (N/m)} \tag{20}$$

$$G = [478350 \;\; 478350 \;\; 517790]^{\text{T}} \text{ (kg)} \tag{21}$$

$$H = \begin{bmatrix} 1 & -1 & 0 \\ 0 & 1 & -1 \\ 0 & 0 & 1 \end{bmatrix} \tag{22}$$

Appendix B
Parameters for the Steady-State LQR and Kalman Gain Syntheses

The control forces and the interstory drift outputs are weighted in the optimized cost of the discrete-time LQR synthesis. The weighting matrices are given in the following, in which Q weighs the interstory drifts, and R weighs the control forces

$$Q = I_{3\times 3}, \quad R = 4.0\text{e}-17 \times I_{3\times 3}. \tag{23}$$

The assumed process noise covariance, W, and the measurement noise covariance, V, for the discrete-time Kalman estimator design are given as follows:

$$W = 1, \quad V = 7.2\text{e}-6 \times I_{3\times 3}. \tag{24}$$

Appendix C
LQGswitch Scenario

The estimator has the correction-propagation form as follows.

Correction:

$$\hat{x}[k|k] = \hat{x}[k|k-1] - E_{\alpha[k]}(C_{\text{d},\alpha[k]}\hat{x}[k|k-1] + D_{\text{d},\alpha[k]}u[k] - y_{\text{r}}^{*}[k]). \tag{25}$$

Propagation:

$$\hat{x}[k+1|k] = A_{\text{d}}\hat{x}[k|k] + B_{\text{d}}u[k] \tag{26}$$

where $\hat{x}[k|k]$ and $\hat{x}[k|k-1]$ are the estimates of $x(t)$ during the kth time step. $\hat{x}[k|k]$ uses the measurements up to the kth time step, while $\hat{x}[k|k-1]$ uses the measurements only up to the $(k-1)$th time step. $\alpha[k] \in \{1, 2, \ldots, n_{\text{m}}\}$ denotes the Markov mode of the controller at time k. $(A_{\text{d}}, B_{\text{d}}, C_{\text{d},\alpha[k]}, D_{\text{d},\alpha[k]})$ is the discrete-time state-space model of the plant used for Kalman estimator design. $A_{\text{d}} = e^{AT_{\text{s}}}$, $B_d = \int_0^{T_{\text{s}}} e^{A\tau}B_2 \, d\tau$, $C_{\text{d},\alpha[k]}$, and $D_{\text{d},\alpha[k]}$ are formed from the rows of C_y and D_y that connect to the remaining measurements. When a subset of the measurements is lost, the estimator will perform the correction step using only the remaining measurements, $y_{\text{r}}^{*}[k]$, and the corrector gains, $E_{\alpha[k]}$. $E_{\alpha[k]}$ is obtained from the steady-state Kalman estimator solution of $(A_{\text{d}}, B_{\text{d}}, C_{\text{d},\alpha[k]}, D_{\text{d},\alpha[k]})$.

Initial Conditions: $u[0] = 0$, and $\hat{x}[0|0] = 0$.

The regulator uses $\hat{x}[k+1|k]$ to compute the control forces to be applied during the $(k+1)$th time step

$$u[k+1] = -F\hat{x}[k+1|k] \tag{27}$$

where F is the steady-state LQR gain.

APPENDIX D
FORMULATION OF THE LIFTED PLANT

$$A_{\mathrm{s}} = A_{\mathrm{f}}^{N} \tag{28}$$

$$B_{\mathrm{s},1} = \begin{bmatrix} A_{\mathrm{f}}^{N-1}B_{\mathrm{f},1} & A_{\mathrm{f}}^{N-2}B_{\mathrm{f},1} & \cdots & A_{\mathrm{f}}B_{\mathrm{f},1} & B_{\mathrm{f},1} \end{bmatrix} \tag{29}$$

$$B_{\mathrm{s},2} = A_{\mathrm{f}}^{N-1}B_{\mathrm{f},2} + A_{\mathrm{f}}^{N-2}B_{\mathrm{f},2} + \cdots + A_{\mathrm{f}}B_{\mathrm{f},2} + B_{\mathrm{f},2} \tag{30}$$

$$C_{\mathrm{s},z} = \begin{bmatrix} C_z \\ C_zA_{\mathrm{f}} \\ \cdots \\ C_zA_{\mathrm{f}}^{N-1} \end{bmatrix} \tag{31}$$

$$D_{\mathrm{s},z1} = \begin{bmatrix} 0 & 0 & \cdots & \cdots & 0 \\ C_zB_{\mathrm{f},1} & 0 & \cdots & \cdots & 0 \\ C_zA_{\mathrm{f}}B_{\mathrm{f},1} & C_zB_{\mathrm{f},1} & \ddots & \cdots & 0 \\ \vdots & \vdots & \vdots & \ddots & \vdots \\ C_zA_{\mathrm{f}}^{N-2}B_{\mathrm{f},1} & C_zA_{\mathrm{f}}^{N-3}B_{\mathrm{f},1} & \cdots & \cdots & 0 \end{bmatrix} \tag{32}$$

$$D_{\mathrm{s},z2} = \begin{bmatrix} 0 \\ C_zB_{\mathrm{f},2} \\ C_zA_{\mathrm{f}}B_{\mathrm{f},2} + C_zB_{\mathrm{f},2} \\ \vdots \\ C_zA_{\mathrm{f}}^{N-2}B_{\mathrm{f},1} + \cdots + C_zA_{\mathrm{f}}B_{\mathrm{f},2} + C_zB_{\mathrm{f},2} \end{bmatrix}. \tag{33}$$

APPENDIX E
PROBABILITY DISTRIBUTION OF THE JUMPING MODES OF LQRONOFF, LQRHOLD, AND LQGSWITCH

$\alpha[k]$ (or i)	$\theta[k]$	v_i
1	$[0,0,0]^{\mathrm{T}}$	p^3
2	$[1,0,0]^{\mathrm{T}}$	$p^2(1-p)$
3	$[0,1,0]^{\mathrm{T}}$	$p^2(1-p)$
4	$[1,1,0]^{\mathrm{T}}$	$p(1-p)^2$
5	$[0,0,1]^{\mathrm{T}}$	$p^2(1-p)$
6	$[1,0,1]^{\mathrm{T}}$	$p(1-p)^2$
7	$[0,1,1]^{\mathrm{T}}$	$p(1-p)^2$
8	$[1,1,1]^{\mathrm{T}}$	$(1-p)^3$

$\alpha[k]$ (or i) indexes the Markov mode, $\theta[k]$ describes the loss/receipt for each floor, for example, $\theta(k) = [1,0,0]^{\mathrm{T}}$ corresponds to receiving only the first floor, v_i is the probability of the ith Markov mode, and p is the probability of signal loss of an individual channel.

REFERENCES

[1] G. W. Housner *et al.*, "Structural control: Past, present, and future," *J. Eng. Mech.*, vol. 123, no. 9, pp. 897–971, 1997, doi: 10.1061/(ASCE)0733-9399(1997)123:9(897).

[2] B. F. Spencer and S. Nagarajaiah, "State of the art of structural control," *J. Struct. Eng.*, vol. 129, no. 7, pp. 845–856, 2003, doi: 10.1061/(ASCE)0733-9445(2003)129:7(845).

[3] Y. Wang, R. A. Swartz, J. P. Lynch, K. H. Law, K.-C. Lu, and C.-H. Loh, "Decentralized civil structural control using real-time wireless sensing and embedded computing," *Smart Struct. Syst.*, vol. 3, no. 3, pp. 321–340, Jul. 2007.

[4] R. A. Swartz and J. P. Lynch, "Strategic network utilization in a wireless structural control system for seismically excited structures," *J. Struct. Eng.*, vol. 135, no. 5, pp. 597–608, 2009, doi: 10.1061/(ASCE)ST.1943-541X.0000002.

[5] J. P. Lynch, "A summary review of wireless sensors and sensor networks for structural health monitoring," *Shock Vib. Dig.*, vol. 38, no. 2, pp. 91–128, Mar. 2006.

[6] N. Sandell, P. Varaiya, M. Athans, and M. Safonov, "Survey of decentralized control methods for large scale systems," *IEEE Trans. Autom. Control*, vol. 23, no. 2, pp. 108–128, Apr. 1978.

[7] B. D. Winter and R. A. Swartz, "Communication patterning for multi-step TDMA bandwidth allocation using wireless structural control," in *Proc. Amer. Control Conf. (ACC)*, Jul. 2016, pp. 6345–6350.

[8] B. D. Winter and R. Andrew Swartz, "Wireless structural control using stochastic bandwidth allocation and dynamic state estimation with measurement fusion," *Struct. Control Health Monitor.*, vol. 25, no. 2, p. e2104, Feb. 2018. [Online]. Available: https://onlinelibrary.wiley.com/doi/abs/10.1002/stc.2104

[9] L. E. Linderman and B. F. Spencer, "Decentralized active control of multistory civil structure with wireless smart sensor nodes," *J. Eng. Mech.*, vol. 142, no. 10, 2016, Art. no. 04016078, doi: 10.1061/(ASCE)EM.1943-7889.0001126.

[10] H. Soury, T. H. T. Truong, L. Linderman, and B. Smida, "Impact of multiple access technique on wireless structural control," in *Proc. 13th Int. Wireless Commun. Mobile Comput. Conf. (IWCMC)*, Jun. 2017, pp. 1201–1208, doi: 10.1109/IWCMC.2017.7986456.

[11] K. Gatsis, H. Hassani, and G. J. Pappas, "Latency-reliability tradeoffs for state estimation," 2018, *arXiv:1810.11831*. [Online]. Available: http://arxiv.org/abs/1810.11831

[12] B. Li *et al.*, "Realistic case studies of wireless structural control," in *Proc. ACM/IEEE 4th Int. Conf. Cyber-Phys. Syst. (ICCPS)*, Apr. 2013, pp. 179–188.

[13] Z. Sun, G. Ou, S. J. Dyke, and C. Lu, "A state estimation method for wireless structural control systems," *Struct. Control Health Monitor.*, vol. 24, no. 6, p. e1929, Jun. 2017. [Online]. Available: https://onlinelibrary.wiley.com/doi/abs/10.1002/stc.1929

[14] S. C. Smith and P. Seiler, "Estimation with lossy measurements: Jump estimators for jump systems," *IEEE Trans. Autom. Control*, vol. 48, no. 12, pp. 2163–2171, Dec. 2003.

[15] P. J. Seiler, "Coordinated control of unmanned aerial vehicles," Ph.D. dissertation, Dept. Mech. Eng., Univ. California, Berkeley, CA, USA, Jan. 2001.

[16] R. Lozano, N. Chopra, and M. Spong, "Passivation of force reflecting bilateral teleoperators with time varying delay," in *Proc. 8th Mechatronics Forum*, 2002, pp. 24–26.

[17] S. Stramigioli, C. Secchi, A. J. van der Schaft, and C. Fantuzzi, "Sampled data systems passivity and discrete port-Hamiltonian systems," *IEEE Trans. Robot.*, vol. 21, no. 4, pp. 574–587, Aug. 2005.

[18] H. Tajimi, "A statistical method for determining the maximum response of a building structure during an earthquake," in *Proc. 2nd World Conf. Earthquake Eng.*, 1960, pp. 781–797.

[19] B. F. Spencer, S. J. Dyke, and H. S. Deoskar, "Benchmark problems in structural control: Part I—Active mass driver system," *Earthq. Eng. Struct. Dyn.*, vol. 27, no. 11, pp. 1127–1139, 1998, doi: 10.1002/(SICI)1096-9845(1998110)27:11<1127::AID-EQE774>3.0.CO;2-F.

[20] O. L. D. V. Costa, M. D. Fragoso, and R. P. Marques, *Discrete-Time Markov Jump Linear Systems*. London, U.K.: Springer, 2000.

[21] B. Bamieh, J. B. Pearson, B. A. Francis, and A. Tannenbaum, "A lifting technique for linear periodic systems with applications to sampled-data control," *Syst. Control Lett.*, vol. 17, no. 2, pp. 79–88, Aug. 1991.

[22] T. Chen and B. A. Francis, *Optimal Sampled-Data Control Systems*. London, U.K.: Springer, 1995. [Online]. Available: http://link.springer.com/10.1007/978-1-4471-3037-6

[23] G. N. Bycroft, "White noise representation of earthquakes," *J. Eng. Mech. Division*, vol. 86, no. 2, pp. 1–16, 1960.

[24] G. F. Franklin, D. J. Powell, and A. Emami-Naeini, *Feedback Control of Dynamic Systems*, 4th ed. Upper Saddle River, NJ, USA: Prentice-Hall, 2001.

[25] P. Seiler and R. Sengupta, "Analysis of communication losses in vehicle control problems," in *Proc. Amer. Control Conf.*, vol. 2, Jun. 2001, pp. 1491–1496.

[26] Y. Ohtori, R. E. Christenson, B. F. Spencer, and S. J. Dyke, "Benchmark control problems for seismically excited nonlinear buildings," *J. Eng. Mech.*, vol. 130, no. 4, pp. 366–385, 2004, doi: 10.1061/(ASCE)0733-9399(2004)130:4(366).

[27] R. J. Guyan, "Reduction of stiffness and mass matrices," *AIAA J.*, vol. 3, no. 2, p. 380, 1965, doi: 10.2514/3.2874.

[28] Y. Ji, H. J. Chizeck, X. Feng, and K. A. Loparo, "Stability and control of discrete-time jump linear systems," *Control-Theory Adv. Technol.*, vol. 7, no. 2, pp. 247–270, 1991.